

# Tomographic Image Reconstruction from a Sparse Projection Data Using Sinogram Interpolation

Catur Edi Widodo, Kus Kusminarto, Gede Bayu Suparta

**Abstract** - In this paper we propose a new approach of tomographic image reconstruction using sinogram interpolation for a sparse projection data. In this term, sinogram interpolation is a process of converting a sampled projection to a higher sampling rate projection. By using interpolation, we construct a new projections within the range of set of projection, then we apply a filtered backprojection reconstruction to get the tomographic image. This proposed approach reconstruction is applied to simulated half full angle projection data of the Shepp-Logan phantom with sparse angular sampling. The result are better than those given by filtered backprojection reconstruction without sinogram interpolation.

**Keyword** - tomography, projection, sinogram, interpolation, backprojection

## I. INTRODUCTION

In tomography, the inner structure of object is reconstructed from a collection of projection data. The widely used computerized tomography (CT) imaging uses an extensive set of projections acquired from all around the body. Reconstruction from such complete data is by now well understood, most popular method being filtered back-projection [1]. In medical tomography, it is important to consider the dose received by patient because the greater the radiation dose, the greater the risk of tissue damage and the risk of cancer [2], [3].

Many strategies have been proposed to reduce dose by minimizing radiation exposure but using low dose may result quantum noise [2]. This quantum noise can be reduced by applying suitable filter on sinogram from scanning object. Bharkada et. al. [4] reduce dose radiation by applying normal dose for region of interest (ROI) object and applying very low dose for non ROI object. The widely used method to reduce dose is by reducing the number of projections by widening the projection angel interval. We refer to this types of incomplete data as *sparse projection data*. The weakness of this method is in the image reconstruction results will arise an artefact defect. By using the evolution theory [1], wavelet transform [3], convex projection method [5], total variation [6], and metric labeling [7], reconstruction can be done without causing artefact defect using ten projections only.

All works we have described above are iterative methods. This method is based on idea of solving a system of linear equations in which the linear attenuation coefficient distribution of the object,  $\mu(x,y)$ , and its projection,  $p_\theta(x_r)$ , are considered as discrete matrices,  $M$

and  $P$ , respectively. These two matrices are related by  $P = RM$ , when  $R$  is a matrix transformation that describes the Radon transform operation. The objective is then to find the inverse transform operator,  $R^{-1}$  [8]. All iterative methods commence from initial guess for  $M_0$ . From this the projections,  $P$ , are determined and compared to experimental values of  $P_{exp}$ . The projection errors is then used to form a corrected projection set which is subsequently used to produce the new value of  $M_1$ . In the algebraic reconstruction technique (ART), the projection error used to correct projection is exactly  $\Delta P = P_{exp} - P$ , but in further technique (partly we describe above is convex projection, evolution theory, and total variation) is determined by statistical consideration. The aim of our work is to propose a new approach, where we do interpolate the sinogram with sparse projection then perform backprojection to get the reconstructed image.

## II. ALGORITHM

The Radon Transform has several useful properties [9] (Table 1). The property of linearity can be described as follow: Suppose there are  $N$  objects, each of object has the functions of  $f_1(x,y), f_2(x,y), \dots, f_n(x,y)$ , and each function is multiplied by the scalar  $a_1, a_2, \dots, a_n$ , the Radon transform of linear combination all of these functions is same as linear combination of each of its Radon transform. The projections  $g(s, \theta)$  are space limited in  $s$  if the object  $f(x,y)$  is space limited in  $(x,y)$ , and they are periodic in  $\theta$  with period  $2\pi$ . A translation of  $f(x,y)$  results in the shift of  $g(s,\theta)$  by a distance equal to the projection of the translation vector on the line  $s = x \cos \theta + y \sin \theta$ . A rotation of the object by an angle  $\theta$  causes a translation of its Radon transform in the variable  $\theta$ . A scaling of the  $(x,y)$  coordinates of  $f(x,y)$  results in scaling of the  $s$  coordinate together with an amplitude scaling of  $g(s,\theta)$ . Finally, the total mass of distribution  $f(x,y)$  is preserved by  $g(s,\theta)$  for all  $\theta$ .

Table I  
Properties of Radon Transform [9]

No.	Function	Radon Transform
1	$f(x, y) = f_r(r, \phi)$	$g(s, \theta)$
2	Linearity: $a_1 f_1(x, y) + a_2 f_2(x, y)$ Space limitedness: $f(x, y) = 0,  x  > \frac{D}{2},  y  > \frac{D}{2}$	$a_1 g_1(s, \theta) + a_2 g_2(s, \theta)$ $g(s, \theta) = 0,  s  > \frac{D\sqrt{2}}{2}$
3	Symmetry: $f(x, y)$	$g(s, \theta) = g(-s, \theta \pm \pi)$
4	Periodicity: $f(x, y)$	$g(s, \theta) = g(s, \theta + 2k\pi), k = \text{integer}$
5	Shift: $f(x - x_0, y - y_0)$	$g(s - x_0 \cos \theta - y_0 \sin \theta, \theta)$
6	Rotation by $\theta_0$ : $f_r(r, \phi + \theta_0)$	$g(s, \theta + \theta_0)$
7	Scaling: $f(ax, ay)$	$\frac{1}{ a } g(as, \theta), a \neq 0$
8	Mass conservation: $M = \iint_{-\infty}^{\infty} f(x, y) dx dy$	$M = \int_{-\infty}^{\infty} g(s, \theta) ds, \forall \theta$

According to the properties of linearity, a point in Cartesian space corresponds to a sine pattern in the radon space. If there are N points in Cartesian space, it will correspond with the N sine pattern in the radon space. If there are points forming the object in Cartesian space, it corresponds to a sine band on Radon space. If there are several objects in Cartesian space, it there will correspond several sine bands on Radon space. So if there are sparse data on radon space, missing data can be filled by way of interpolation in order to form a sine bands. Gray level of the sine band is determined from the properties of conservation of mass that is total gray level of each projection is the same, so that the gray level of each of the coordinates can be interpolated.

Unlike a widely used interpolation, where interpolation is only done on a gray level with a predetermined position, the proposed interpolation is done on the position and gray level. Illustration of the interpolation process that we are proposed can be seen in Fig. 1, 2 and 3.

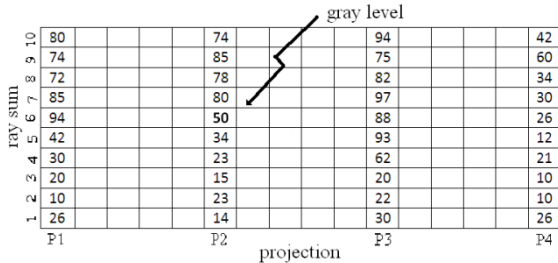


Fig. 1. Example of projections that will be interpolated

Suppose we are in a position to projection P2 on 6<sup>th</sup> raysum with gray level 50. At P1, the closest gray level to 50 is 42 which is at 5<sup>th</sup> raysum. At P3, the closest gray level to 50 is 62 which is at 4<sup>th</sup> raysum. At P4, the closest gray levels to 62 is 60, which is at 9<sup>th</sup> raysum. Based on these data we obtain the set of raysum positions P1, P2, P3 and P4 to be interpolated, there are (5,6,4,9). Then we do 1- dimension spline interpolation to these data to produce 16 data sets of interpolation values, there are (5, 6, 6, 6, 6, 6, 5, 5, 4, 4, 4, 4, 5, 6, 7, 9). Data are selected to fill raysum between P2 and P3 is the data at 7<sup>th</sup>, 8<sup>th</sup>, 9<sup>th</sup> and 10<sup>th</sup>, there are (5,5,4,4) as can see in Fig. 2 (these positions are marked with the symbol  $\surd$ ).

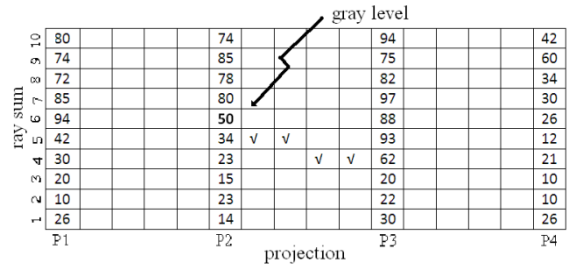


Fig. 2. Position interpolation for projection P2 on 6<sup>th</sup> raysum

To determine the gray level on raysum which have been obtained, we take gray level on raysum at P1=5<sup>th</sup>, P2=6<sup>th</sup>, P3=4<sup>th</sup> and P4=9<sup>th</sup>, there are (42,50,62,60). Then we do 1-dimension spline interpolation to these data to produce 16 data sets of interpolation values, there are (42, 44, 45, 47, 48, 50, 52, 55, 57, 60, 62, 62, 61, 60, 60, 60). Gray level data selected to fill positions that have been previously obtained is the data at 7<sup>th</sup>, 8<sup>th</sup>, 9<sup>th</sup> and 10<sup>th</sup>, there are (52,55,57,60).

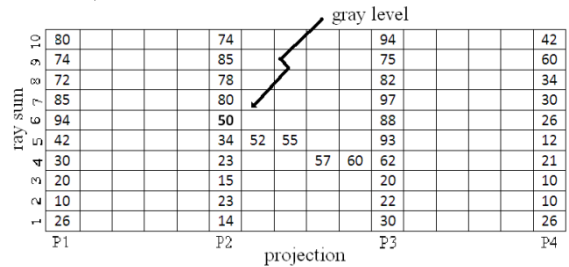


Fig. 3. Interpolation result for projection P2 on 6<sup>th</sup> raysum

To implement this algorithm, the projections are arranged in order of P0, P1, P2, ..., Pn, Pn +1, where P0 is Pn with a reversed raysum sequence; P1, P2, ... Pn is the 1<sup>st</sup>, 2<sup>nd</sup>, ... n<sup>th</sup> projection; and Pn +1 is P1 with a reversed raysum sequence.

Below is the proposed sinogram interpolation algorithm:

1. Get the projections P1 and P2
2. Determine the points of interpolation by steps:
  - for i = 1 to N
    - left=i
    - nleft=P2(i)
    - for k=1 to M
      - PN<sub>k</sub> = absolute (P2<sub>left</sub> - P1<sub>k</sub>)
    - endfor
    - for k=1 to M
      - if PN<sub>k</sub> = minimum (PN)
      - outleft=k
      - noutleft=P1(k);
      - endif
    - endfor
    - for k=1 to M
      - PN<sub>k</sub> = absolute (P2<sub>left</sub> - P3<sub>k</sub>)
    - endfor
    - for k=1 to M
      - if PN<sub>k</sub> = minimum (PN)
      - right=k
      - nright=P3(k);
      - endif
    - endfor
    - for k=1 to M
      - PN<sub>k</sub> = absolute (P3<sub>right</sub> - P4<sub>k</sub>)
    - endfor
    - for k=1 to M
      - if PN<sub>k</sub> = minimum (PN)
      - outright=k
      - noutright=P4(k);

```

        endif
    endfor
endfor
3. Perform interpolation
4. Fill projections between P1 and P2
5. Return to step 1 for the projections:
   between P2-P3,P3-P4, P4-P5, ... ,PN-PN-1
    
```

### III. EXPERIMENT RESULT

The experiment was conducted as follow: We simulated various sparse projection data using the synthetic Shepp-Logan phantom of size 256 X 256 generated by MatLab as shown in Fig. 4. The test case is a simulated example of half full angle tomography of sparse projection data with angular step of 5° (36 projections), 10° (18 projections), 15° (12 projections), 20° (9 projections), 25.7° (7 projections), and 30° (6 projections). We are interpolated these sparse projections to construct sinogram of 360 projections. We chose this 360 projections because it is suitable to interpolate (can be divided by 5, 10, 15, 20 and 30) and conform the sampling theory [10], where  $M_{projection} \approx \frac{1}{2}\pi N_{raysum}$ . From this sinogram we do backprojection reconstruction. We studied the effect of angular sampling on reconstruction quality using signal to noise (SNR) criterion by formula:

$$SNR (dB) = 10 \log_{10} \left( \frac{\sum_{i,j} x(i, j)^2}{\sum_{i,j} (x(i, j) - y(i, j))^2} \right)$$



Fig. 4. Synthetic Shepp-Logan Phantom generated by MatLab

Simulation result can be seen in Fig. 5 where visually shows that there is no streak artifact on the reconstructed image with interpolation sinogram (fifth column). The less number of projection, the lower the quality of the resulting image, and the more different the reconstructed image with the original image. This is due to the closest gray level is not necessarily the actual direction. To get better results, each gray level obtained from the interpolation should be checked whether it is in the right direction.

Nevertheless, with only nine projections, small objects can still be identified so that the reconstruction is still acceptable. In quantitative terms, the proposed interpolation can significantly increases the SNR in both sinogram and reconstructed image (Fig.6 and Fig.7).

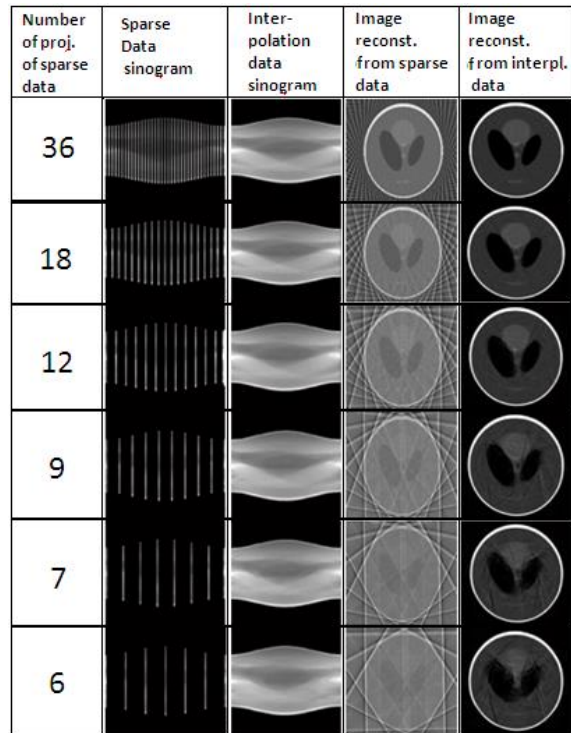


Fig. 5. Simulated sparse half full angle projection data from the Shepp-Logan phantom. First column from the left: number of projection of sparse data. In all cases the total view angle is 180°. The number of projections from top to bottom are 36 (5° step), 18 (10° step), 12 (15° step), 9 (20° step), 7 (25.7° step), and 6 (30° step), respectively. Second column: data sampled projection in sinogram form. The missing parts of the sinograms are denoted by black. Third column: interpolated sinogram. Forth column: reconstructions using filtered backprojection without sinogram interpolation. Fifth column: reconstructions using filtered backprojection with sinogram interpolation.

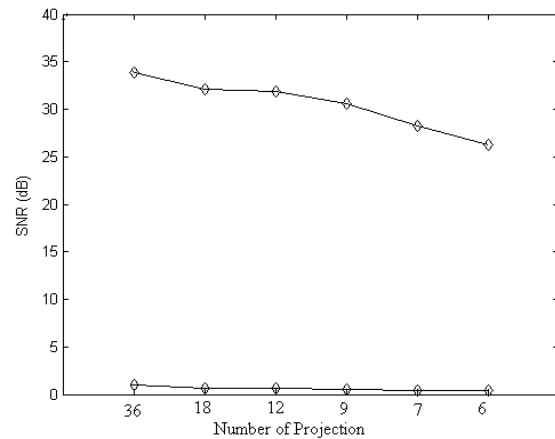


Fig. 6. Graphic of SNR of sinogram versus number of projection. Curve below: sparse projections. Curve above: interpolated projections

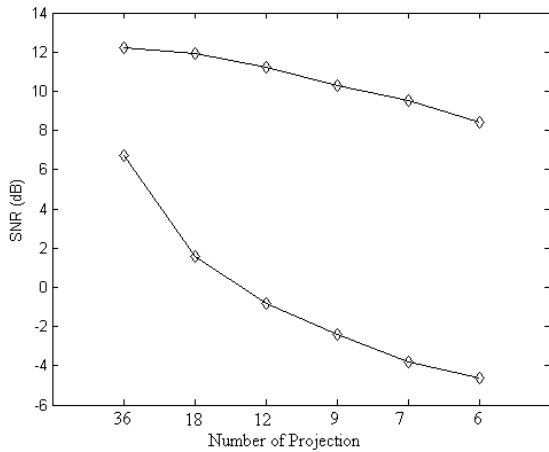


Fig. 7. Graphic of SNR of reconstruction image versus number of projection. Curve below: reconstruction using filtered backprojection without sinogram interpolation. Curve above: reconstruction using filtered backprojection with sinogram interpolation

#### IV. CONCLUSION

In this work, a method of sinogram interpolation has been developed. The method increases significantly values of SNR of sinogram and reconstructed image. Visually, the results of reconstruction with the proposed approach indicates no streak artefact. On a phantom Shepp-Logan object, the reconstruction is acceptable by using nine projections only.

#### REFERENCES

- [1] V. Kolehmainen, M. Lassas, and S. Siltanen, 2008, Limited Data X Ray Tomography Using Nonlinear Evolution Equations, *SIAM Journal of Scientific Computation*, p.p. 1413-1429
- [2] J. Wang, H. Lu, J. Wen, and Z. Liang, 2006, Multiscale Penalized Weighted Least-Squares Sinogram Restoration for Low-Dose X-Ray Computed Tomography, *Conf Proc IEEE Eng Med Biol Soc*.
- [3] H. Yu, and G. Wang, 2010, SART-Type Image Reconstruction from a Limited Number of Projection with the Sparsity Constraint, *Int. Jour. of Biomedical Imaging*, Vol 2010, Article ID 934847.
- [4] D. Bharkhada, H. Yu, G. Shuping, J.J. Carr and G. Wang, 2009, Cardiac Computed Tomography Radiation Dose Reduction Using Interior Reconstruction Algorithm With the Aorta dan Vertebra as Known Information, *J. Comput. Assist. Tomogr.*, Volume 33, Number 3.
- [5] P. Oskoui-Fard and H. Stark, 1988, Tomographic Image Reconstruction Using the Theory of Convex Projection, *IEEE Trans. Med. Imag.*, Vol 7, p.p. 45-58
- [6] G.T. Herman, and R. Davidi, 2008, Image Reconstruction from a Small Number of Projection, *Inverse Problem*, Vol 24, no. 4.
- [7] V. Singh, L. Mukherjee, J. Xu, and K.R. Hoffmann, 2008, Limited View CT Reconstruction and Segmentation via Constrained Metric Labeling, *CVIU*, Vol 112 no 1 October 2008, p.p 67-80.
- [8] G.B. Suparta, 1999, Focusing Computed Tomography Scanner, *Thesis Ph.D.*, Monash University, Australia.
- [9] K.A. Jain, 1989, *Fundamentals Digital Imaging Processing*, Prentice Hall, New Jersey.
- [10] A.C. Kak and M. Slaney, 1999, *Computerized Tomographic Imaging*, The Institute of Electrical and Electronics Engineers, Inc., New York.

**Catur Edi Widodo** is the Ph.D. candidates in Physics Department, Faculty of Mathematics and Natural Science, Gadjah Mada University, Yogyakarta, Indonesia, and also with the Physics Department, Faculty of Mathematics and Natural Science, Diponegoro University, Semarang, Indonesia (e-mail: catur.ediwidodo@gmail.com).

**Kus Kusminarto** is with the Physics Department, Faculty of Mathematics and Natural Science, Gadjah Mada University, Yogyakarta, Indonesia (e-mail: kusmin@ugm.ac.id)

Gede Bayu Suparta is with the Physics Department, Faculty of Mathematics and Natural Science, Gadjah Mada University, Yogyakarta, Indonesia (e-mail: gbsuparta@ugm.ac.id)